Thermal and Mechanical Analysis of Novel Transcranial Magnetic Stimulation Coil for Mice

S. D. March[1], S. Stark[1], R. L. Hadimani[1], D. R. Stiner[1], M. Senter[1], K. Spoth[1], L. J. Crowther[1], and D. C. Jiles[1], *Fellow, IEEE*

[1]Department of Electrical and Computer Engineering, Iowa State University, Ames, IA 50011 USA

Transcranial Magnetic Stimulation (TMS) has potential to treat various neurological disorders non-invasively and safely. There has been significant work on coil designs for use on the human brain; however, there are fewer reports on the coil design for small animal brains, such as mice. Such work is essential to validate TMS treatment procedures on animals prior to clinical trials. We report thermal and mechanical analysis of a new small-animal coil system designed to produce focused electric fields resulting in more selective deep-brain stimulation. Thermal and magnetic force analyses conducted at experimental TMS operating conditions are used to determine the mechanical stability of the new coil system. Low magnetic linear attraction and rotational forces suggest mechanical stability of the coil. Small temperature increase over a simulated 60-second TMS therapy session indicate the coil system operates within safe temperature limits. This coil configuration can be used on mice to stimulate selective regions of the brain to study various neurological disorders, such as Parkinson's disease.

***Index Terms*—Animal coils, Deep-brain stimulation, Force analysis, Thermal analysis, Transcranial magnetic stimulation (TMS)**

I. Introduction

Transcranial magnetic stimulation (TMS) offers promising non-invasive, surgery-free medical treatment of neurological ailments, such as depression, Parkinson's disease, or Post Traumatic Stress Disorder (PTSD), several of these conditions originating from irregular neurological activity from deep regions of the brain [1, 2]. Existing TMS coils are limited by non-focal electric field profiles and rapid electric field profile strength attenuation within a few centimeters of the brain's surface [3], thus inhibiting the treatment of deep-brain conditions. In several human coil designs, focality is a tradeoff for field strength [4].

The United States Food and Drug Administration (FDA) approved TMS therapy to treat depression after successful human trials, without animal safety data. This has led many to question the ethics and necessity for animal trials at all to test TMS therapy [1]. This apparent "success" was attained by reduced levels in accidental seizures to an accepted level; however, depression has been linked to the amygdala, thalamus, and hippocampus regions of the brain, all of which are far below the brain surface (therefore outside the existing efficacy zone for human coils) [5, 6]. As a result, many TMS clinicians use their coils at suboptimal levels because complete knowledge of the neurological science behind TMS has still not been tested [1]. A lack of suitable non-human models has limited the study of TMS's efficacy and possibility for widespread adoption as a standard neurological treatment procedure. Furthermore, new ailments cannot be treated with TMS coils without successfully conducting animal trials and receiving FDA clearance.

Mice provide a suitable, non-human model to test TMS efficacy due to the extensive medical documentation. Previous work by the authors explored a new small animal coil design for mice [7]. The new design showed strong, focused electric field profiles inside a heterogeneous MRI derived model of a mouse brain after optimizing coil geometry through focality analysis technique developed by Deng *et al.* [8] and electric field profile strength. A progression of final design iterations is given in Fig. 1.

Further work, however, is needed to validate the new coil design in view of physical concerns, such as strong magnetic forces between TMS coils placed in close proximity to each other resulting in large torques and high internal stress. George and Belmaker estimate the magnetic torque experienced by a TMS coil when used in combination with an MRI generating a 1.5 T magnetic field to be 60 Nm [3]. Work by Crowther, *et al.* observed mechanical stress values as high

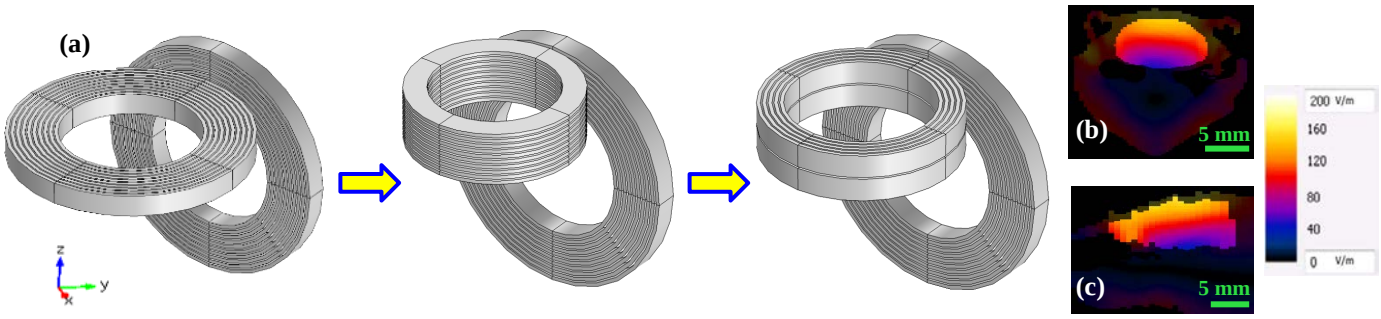

Fig. 1 (a) Progression of coil design iterations incorporating realistic spacing with last coil as the final design. (b) Electric field profile for final coil design on coronal plane at AP = 0 (anterior-posterior) with respect to the bregma. (c) Medial sagittal electric field profile for final coil design. Note, the brain matter in (b) and (c) is highlighted and the surrounding non-brain matter is dimmed for clarity.

as 2.8 × 10^9 Nm^{-3} inside the coils which can potential produce cracks in the coil [9, 10].

Furthermore, the high currents used for TMS therapy could produce dangerous levels of Joule heating that could injure an animal by overheating. Several coil systems incorporate active cooling to regulate coil thermal output. Thermal evaluation of existing neurological treatments is limited to electrode implants [4]. We have developed thermal analysis technique that tests the stability and engineering limits of TMS coil design.

The high current, high magnetic fields, and small dimensions create physical concerns that can lead to mechanical and thermal instabilities. Work by Cohen and Cuffin suggest heat and mechanical concerns cannot be easily surmounted, resulting in a lack of miniaturized mouse coil design and characterization [11]. In this study, we consider unexplored thermal and mechanical responses of miniaturized animal coils by analyzing our new coil system. Force and thermal evaluations were performed under the anticipated TMS operating conditions to identify and mitigate potential design problems and safety concerns.

II. Coil and Helmet System

The coil design considered is composed of several circular copper wire loops with wire cross section of 0.8 × 5.0 mm. The design is separated into two coil groupings, a "horizontal" and "vertical" coil, as shown in Fig. 2. Both coils have 10 turns with outer radii 37. 2 and 31.2 mm for the horizontal and vertical coil, respectively, and are separated by 3.0 mm [7]. To obtain the necessary magnetic field and resulting electric field to induce TMS therapy, coils are pulsed with a 2.5 kHz sinusoidal current pulse train with an amplitude of 5000 A from Magstim Company Ltd. Stimulators. It is established that these parameters are needed to depolarize neurons in the mammalian brain and alter the brain functions safely [12]. Coils designed for small animals require precise coil placement to deliver specific electric and magnetic field profiles in the animal's brain. Existing coil designs are limited in conducting consistent mouse experiments because of the inability to restrain mice sufficiently without anesthesia. The efficacy of TMS cannot be appropriately assessed without generating consistent and reproducible electric and magnetic field profiles. Current methods for restraint include manually holding a mouse both with [13] and without addition restraining tools, such as placing the mouse a transparent cylinder where it is still relatively free to move [14]. Furthermore, existing small animal coils are too large for testing on mice and consequently stimulate the entire body rather than part of the brain [15].

The authors designed a helmet system (Fig. 2) made of glass-ceramic that complements both the physiology of the mouse and the exact positioning of the coils needed to deliver a focused electric and magnetic field into the brain. The mouse considered here is OF1 type mouse whose typical dimensions are: total length of 95mm [16]; head length of 20mm and maximum head diameter of 12mm. The helmet features the ability to rotate, allowing for electric field profile adjustment within the brain, and foam near the mouse's head to secure the mouse position relative to the coils. The addition of the helmet promises consistency of small animal TMS testing; however, the coil system also introduces new physical design considerations, such as thermal response and magnetic force response.

III. Magnetic Force Response

COMSOL's AC/DC module was used for magnetic force simulations. 5000 A DC current was simulated to evaluate the maximum forces anticipated on the coil system. The directions of the currents through the vertical and horizontal coil are parallel at the 90° junction where the coils are closest. Any forces experienced by the coils will directly transfer to the insulation and the helmet, thus the helmet and insulation will hold the coils in place from magnetic forces. The helmet is made of glass-ceramic mica with high mechanical tolerances of 93.1 GPa flexural strength, 276 MPa compressive strength, and 79.3 GPa modulus of elasticity that are significantly

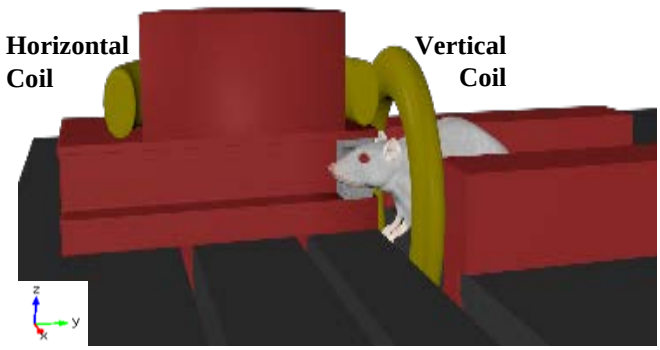

Fig. 2 Side and interior view of coil system with helmet (red) and coils (gold) showing the ability to precisely position mouse relative to coils.

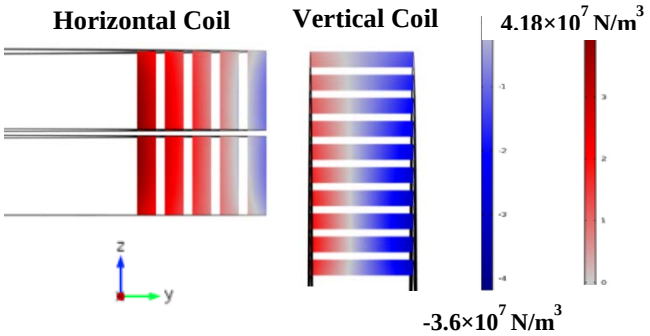

Fig. 3 Interior y-component Lorentz force for coil segment indicating highest internal stress caused by intercoil linear attraction and rotational forces. The cross section is taken on xz plane of figure 1(a) at the center.

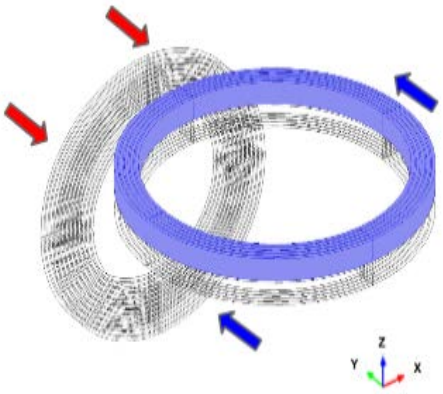

Fig. 4 Example of linear attraction model, where the segment term in equation 2 is the top half of the horizontal coil.

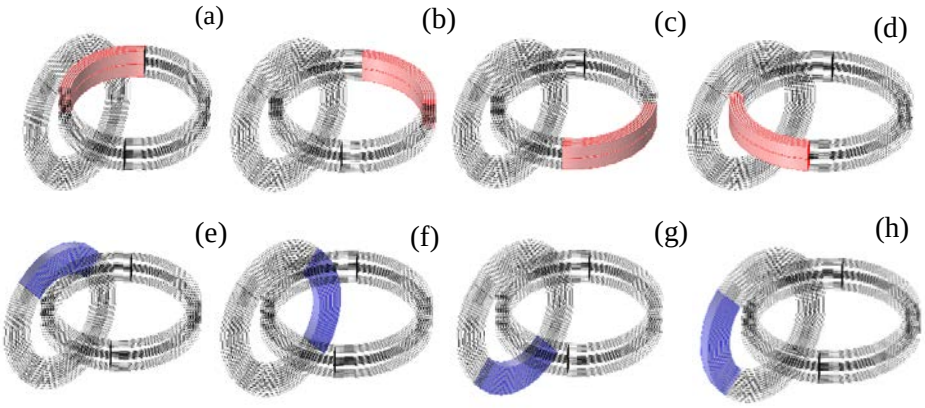

Fig. 5 Segments used for rotational force analysis. For the horizontal coil: (a) segment 1 (b) 2 (c) 3 (d) 4. For the vertical coil: (e) segment 1 (f) 2 (g) 3 (h) 4.

higher than the largest forces produced by the coils [17]

Two forces are considered in this study: linear and rotational magnetic forces. Fig. 3 shows the internal Lorentz force density where the horizontal and vertical coils are closest. A maximum force density value of 4.18×10^7 Nm^{-3} is observed, which is approximately two orders of magnitude lower than the stress reported by Crowther, *et al.* that can potentially cause coil cracking in human coil system [9].

Both the linear and rotational forces are calculated using (1). This is a generalized expression for the force in the *i* direction, where *i* indicates either the x-, y-, or z-directions. The net force given for any segment of coil wire is found by evaluating the volume integral over that segment of wire.

$$\vec{F}_{i,segment} = \iiint d\,\vec{f}_i dV_{segment} \tag{1}$$

Linear attraction between the two coils was modeled by considering the upper and lower layers of the horizontal coil and the vertical coil as rigid structure segments, as shown in Fig. 4. The evaluation of (1) was across the entire circumference of the three coil groupings. Rotational forces are modeled by dividing each coil into quarter loop segments, shown in Fig. 5.

Table I summarizes the magnetic linear attraction forces. The strongest force pulling the coils together acts in the y-direction with a magnitude of 2.56 N (0.575 lbf). Further investigation found the maximum linear attraction force between the upper and lower layers of the horizontal coil is approximately 45 N (10.11 lbf). This data suggests that the coil's mechanical integrity is not affected by linear attraction forces due to the magnetic field.

Table II summarizes the rotational forces experienced by the different quarter segments of the horizontal and vertical coil. The strongest magnitude of rotational force is experienced by the y-components of the horizontal coil with 19.50 N (4.39 lbf) for segment 1 and 10.80 N (2.43 lbf) for segment 3. Also, opposing sides of the horizontal coil show z-component forces acting in opposite directions with 2.40 N (0.54 lbf) for segment 1 and -1.24 N (-0.28 lbf) for segment 3, indicating a rotation, which indicates the presence of a small torque. The strongest magnitude of rotational force experienced by the y-component of segment 1 is 6.35 N (1.43 lbf). Unlike the horizontal coil, the vertical coil forces are axial rather than rotational. The strength of the magnetic rotational forces are too weak to cause significant stress to the coil system.

TABLE I
MAGNETIC LINEAR ATTRACTION FORCE DATA FOR THE VERTICAL AND HORIZONTAL COIL

Coil	Force Direction	Force [N]
Vertical	x	9.72×10^{-5}
	y	-2.63×10^{0}
	z	-6.63×10^{-2}
Horizontal	x	-4.02×10^{-5}
	y	2.27×10^{0}
	z	-1.08×10^{-1}

TABLE II
MAGNETIC ROTATION FORCE DATA FOR THE VERTICAL AND HORIZONTAL COILS BASED ON COIL SEGMENTS

Coil	Segment	x-Force [N]	y-Force [N]	z-Force [N]
Vertical	1	-1.65×10^{-4}	-6.35×10^{0}	1.04×10^{1}
	2	1.17×10^{1}	-1.69×10^{0}	1.72×10^{-1}
	3	-6.70×10^{-6}	-5.13×10^{-1}	-1.10×10^{1}
	4	-1.17×10^{1}	-1.69×10^{0}	1.72×10^{-1}
Horizontal	1	5.77×10^{-5}	1.95×10^{1}	2.40×10^{0}
	2	1.15×10^{1}	3.11×10^{-1}	-1.24×10^{0}
	3	-1.70×10^{-4}	-1.08×10^{1}	-5.31×10^{-1}
	4	-1.15×10^{1}	3.11×10^{-1}	-1.24×10^{0}

IV. THERMAL RESPONSE

High current delivered to the coil is expected to dramatically increase the coil temperature. Gerneral Standard IEC 60601-1 specifies vitreous electronic medical equipment must have a limited surface temperature of of 48 °C [18]. Furthermore, continuous temperature above 150 °C will cause auto-oxidation that degrades the polyurethane insulation that Magstim uses to encase the copper coils [19]. The

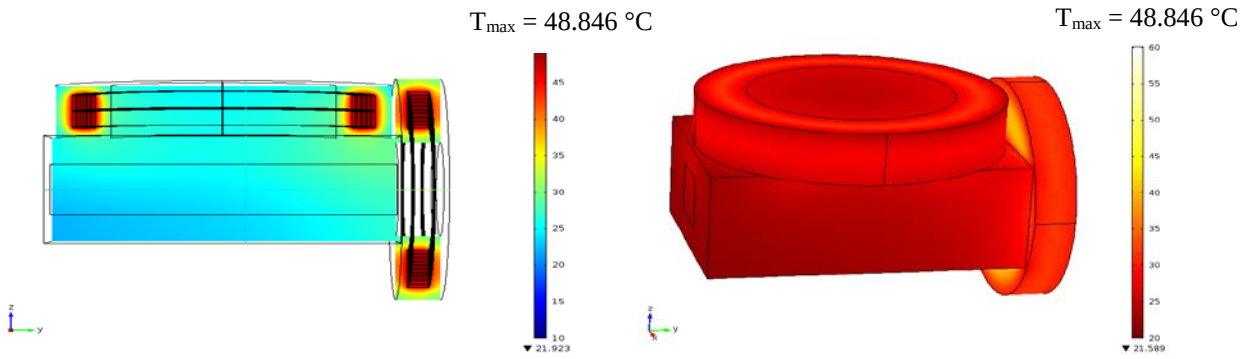

Fig. 6 60 second thermal simulations of coil-helmet system with internal multislice view (left) and external surface view (right) demonstrating safe temperature levels for medical testing.

incompressible Navier-Stokes heat equation from the COMSOL Heat Transfer module, was used to model the thermal changes in the coil system under TMS therapy conditions, as shown in (2),

$$C_p\rho\frac{\partial T}{\partial t}+C_p\rho\vec{u}\bullet\nabla T=\nabla\bullet\left(k\nabla T\right)+Q \tag{2}$$

where ρ is the fluid density, C_p is the fluid heat capacity, T is the temperature, u is the velocity field of the fluid (assumed to be zero), k is the thermal diffusivity of the material, and Q is external source heating.

TABLE III
MATERIAL PARAMETERS USED FOR THERMAL SIMULATIONS

Material	Density [kg-m^{-3}]	Thermal Conductivity [W-m^{-1}-K^{-1}]	Heat Capacity [J-K^{-1}]
Air	1.2	0.02	1047
Copper	8700	400	385
Glass-ceramic Mica	2500	1.15	1400
Polyurethane	1250	0.30	1400
Polyimide	1300	0.15	1100

In the simulation model, the material types used are a solid copper coil encased in a solid insulating layer of polyurethane. The helmet is made of glass-ceramic mica. Both the helmet and the coil are surrounded by air. Convection surface boundary conditions are modeled on all surfaces of the helmet and coil. At t = 0, all materials and surrounding air are set to 20 °C. Material parameters used during thermal simulations are given in Table III.

The Q used during simulation was determined from the anticipated heat produced by the coil given an estimated sinusoidal current pulse and geometry of the coils. All coils share a total length of 1.987 m of copper with a 5.0 mm × 0.8 mm cross section. Assuming a constant resistivity for copper of 1.68 × 10^{-8} Ωm over the anticipated temperature range [20], the resistance of the system is approximately 7.89 × 10^{-3} Ω. A single pulse of current from the stimulators may be approximated as a sinusoidal pulse, given as (3),

$$i(t)=A\sin(2\pi ft) \tag{3}$$

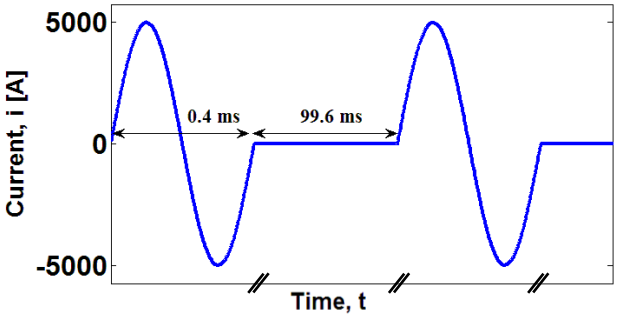

Fig. 7 Segment of current signal pulse train approximation, $i(t)$. The frequency of the pulse is 2.5 kHz with a 100.0 ms period and 0.4 % duty cycle.

where $i(t)$ is the current, A is the signal amplitude of 5000 A, f is the frequency of 2.5 kHz, and t is time. Fig. 7 describes the approximated signal used during simulations. The power generated by the coil is given in (4),

$$P(t)=i(t)^2R \tag{4}$$

where $P(t)$ is the power and R is the resistance of 7.89x10^{-3} Ω. Energy dissipated, Q, for each pulse is determined from (5) by integrating over the 0.4 ms active component of the signal.

$$Q=\int P(t)dt \tag{5}$$

An estimated 78.9 J of heat is generated from each pulse.

To verify the authors' expectations of the simulation model an estimation of the temperature change in the coils was performed. Given the specific heat of copper, c, to be 0.386 Jg^{-1}K^{-1} and the coil mass, m, is found from an assumed density of copper of 8.94 g-cm^{-3}, the temperature change, ΔT, in Q is found to be 1.5 °C per pulse, as determined from (6).

$$Q=cm\Delta T \tag{6}$$

Upon simulation, the observed temperature change in the coil was nearly identical to the predicted 1.5 °C temperature change.

A multislice view and surface temperatures for a 60 second duration of pulse are given in Fig. 6. The minimum temperature in Fig. 6 (left) is 21.9 °C and in Fig. 6 (right) 21.5 °C. The baseline temperature used in the left and right part of the image is 10 and 20 °C respectively. The maximum temperature observed from the multislice view at the boundary between the coils and the polyurethane is 48.85 °C. This is well below the 150 °C polyurethane thermal limitation. The surface temperature is highest on the inner edge of the vertical coil, between 40 °C and 45 °C. This is below the 48 °C IEC requirement and does not require the use of active cooling. We anticipate the addition of active cooling would keep the coil system temperature well below the 48 °C threshold. Both surface and multislice simulations indicate the coil design developed is thermally stable for small-animal TMS therapy administration. Future work will characterize the exact thermal response of the coil.

V. Conclusion

TMS offers a method to treat neurological disorders non-invasively; however, limited human and animal trials leave the efficacy of TMS still relatively unexplored. The design proposed in this study provides a robust platform through which to conduct animal trials. This study successfully investigated the mechanical and thermal stability of a proposed novel coil design. We successfully demonstrated that the design meets physical constraints caused by magnetic linear attraction and rotational forces and temperature increases during TMS therapy when simulated with a high degree of physical accuracy.

Acknowledgment

This work was supported by the Carver Charitable Trust and the Barbara and James Palmer Endowment at the Department of Electrical and Computer Engineering, Iowa State University.

References

[1] E. M. Wassermann and T. Zimmermann, “Transcranial magnetic brain stimulation: therapeutic promises and scientific gaps,” Pharmacology & therapeutics, vol. 133, no. 1, pp. 98–107, Jan. 2012.

[2] E. M. Wassermann and S. H. Lisanby, “Therapeutic application of repetitive transcranial magnetic stimulation: a review,” Clinical Neurophysiology, vol. 112, no. 8, pp. 1367–1377, Aug. 2001.

[3] M. S. George, & R. H. Belmaker, (2000). *Transcranial magnetic stimulation in neuropsychiatry*. Washington, DC: American Psychiatric Press.

[4] S. Rossi, M. Hallett, P. M. Rossini, A. Pascual-Leone, Safety, ethical considerations, and application guidelines for the use of transcranial magnetic stimulation in clinical practice and research. Clinical Neurophysiology, , 120, 2008–39, 2009

[5] E. Irle, M. Ruhleder, C. Lange, U. Seidler-Brandler, S. Salzer , et al,. Reduced amygdalar and hippocampal size in adults with generalized social phobia. Journal of Psychiatry Neuroscience 35, 126–131, 2010.

[6] K. A. Young, L. A. Holcomb, U. Yazandi, P. B. Hicks, D. C. German. Elevated neuron number in the limbic thalamus in major depression. *American Journal of Psychiatry*, 161, 1270-7, 2004

[7] S. D. March, S. McAtee, M. Senter, K. Spoth, D. R. Stiner, L. J. Crowther, R. L. Hadimani, and D. C. Jiles, "Focused and Deep Brain Magnetic Stimulation Using New Coil Design in Mice", Conference proceedings of 6th Neural Engineering Conference, San Diego, 2013.

[8] Zhi-De Deng, Sarah H. Lisanby, Angel V. Peterchev, Electric field depth–focality tradeoff in transcranial magnetic stimulation: Simulation comparison of 50 coil designs, Brain Stimulation, Volume 6, Issue 1, January 2013, Pages 1-13, ISSN 1935-861X, 10.1016/j.brs.2012.02.005.

[9] L. J. Crowther, K. Porzig, R. L. Hadimani, H. Brauer, and D. C. Jiles, Realistically modeled TMS coils for stress and Lorentz force calculations during MRI, IEEE Transactions on Magnetics, vol. 49, no. 7, pp. 3426-3429, 2013.

[10] L. J. Crowther, K. Porzig, R. L. Hadimani, H. Brauer, and D. C. Jiles, "Calculation of Lorentz Forces on Coils for Transcranial Magnetic Stimulation During Magnetic Resonance Imaging," *IEEE Transactions on Magnetics*, vol.48, no.11, pp.4058-4061, Nov 2012.

[11] D. Cohen, B. N. Cuffin. Developing a more focal magnetic stimulator. Part 1: Some basic principles. *Journal of Clinical Neurophysiology*, 8, 102-111, 1991.

[12] G. S. Pell, Y. Roth, and A. Zangen, “Modulation of cortical excitability induced by repetitive transcranial magnetic stimulation: influence of timing and geometrical parameters and underlying mechanisms.,” *Prog. Neurobiol.*, vol. 93, no. 1, pp. 59–98, Jan. 2011.

[13] T. Ikeda, M. Kurosawa, C. Morimoto, S. Kitayama, N. Nukina. “Multiple Effects of Repetitive Transcranial Magnetic Stimulation on Neuropsychiatric Disorders” Biochemical and Biosphysical Research Communications 436, 121 – 127, 2013.

[14] P. Sun, F. Wang, L. Wang, Y. Zhang, R. Yamamoto, T. Sugai, Q. Zhang, Z. Wang, N. Kato. “Increase in Cortical Pyramidal Cell Excitability Accompanies Depression-Like Behavior in Mice: A Transcranial Magnetic Stimulation Study”. The Journal of Neuroscience 31(45), 2011.

[15] M. Hallett,, & S. Chokroverty, *Magnetic stimulation in clinical neurophysiology*. Philadelphia, Pa Elsevier Butterworth-Heinemann, pp. 312-322, 2005.

[16] L. J. Crowther, R. L. Hadimani, A. G. Kanthasamy, and D. C. Jiles, “Transcranial magnetic stimulation of mouse brain using high-resolution anatomical models,” *J. Appl. Phys.*, vol. 115, no. 17, p. 17B303, May 2014. http://dx.doi.org/10.1063/1.4862217

[17] Mykroy/Mycalex Ceramics “Mykroy/Mycalex MM 800 Machining Grade Glass-bonded Mica Composite” 2013. Datasheet.

[18] IEC IS 60601-1: 2005: Medical Electrical Equipment -- Part 1: General Requirements for Basic Safety and Essential Performance. P. 305 – 308.

[19] N. M. K. Lamba, K. A. Woodhouse, S. L. Cooper. “Polyurethanes in Biomedical Applications”, CRC Press, pp. 183-184, Nov. 1997.

[20] D. R. Lide. “Handbook of Chemistry and Physics”, Ed 75. CRC Press, pp. 12-41, 1994.